Posture regulation for unicycle-like robots with prescribed performance guarantees

Martina Zambelli*[1], Yiannis Karayiannidis†[2] and Dimos V. Dimarogonas‡[1]

[1]ACCESS Linnaeus Center and Centre for Autonomous Systems, School of Electrical Engineering, Department of Automatic Control, KTH Royal Institute of Technology, SE-100 44, Stockholm, Sweden.

[2]Computer Vision and Active Perception Lab., Centre for Autonomous Systems, CSC, KTH Royal Institute of Technology, SE-100 44, Stockholm, Sweden.

July 18, 2014

Abstract

This paper aims to address the regulation problem for the unicycle model while guaranteeing prescribed performance. Different controllers based either on polar coordinates or time-varying laws are proposed. The main contribution is the combination of the standard control laws that allow to achieve posture regulation for the unicycle, with the prescribed performance control technique that imposes time-varying constraints to the system coordinates. In order to apply prescribed performance to the unicycle system which is subject to a nonholonomic constraint, we design a specific transformation function that is instrumental in the proof of asymptotic convergence with prescribed guaranties.

1 Introduction

Over the past thirty years wheeled mobile robots (WMRs) have become increasingly important in a wide variety of applications such as transportation, security, inspection, planetary

*zambelli@kth.se

†yiankar@kth.se

‡dimos@kth.se

exploration, etc. WMRs are increasingly present in industrial and service robotics, particularly when flexible motion capabilities are required. The most common for single-body robots are differential drive and synchro drive (both kinematically equivalent to a unicycle), tricycle or car-like drive, and omnidirectional steering.

Beyond the relevance in applications, the problem of control of WMRs has certain theoretical challenges. In particular, these systems are typical examples of nonholonomic mechanisms due to the perfect rolling constraints on the wheel motion (no longitudinal or lateral slipping). With respect to the control of nonholonomic systems, one of the technical hurdles often cited is that the regulation problem cannot be solved via a smooth, time-invariant state feedback law due to the implications of Brockett's condition [1]. There exist different approaches to control a nonholonomic system, such as a unicycle-like robot. See for example [2] for discontinuous control, [3] for dynamic feedback linearization technique, [4] for discontinuous backstepping, [5] for an approach involving an appropriate potential function, [6, 7] for nonlinear control laws constructed using Lyapunov stability analysis, [8] for chained form systems control and time-varying point-stabilization, [9] for control with polar coordinate, and also [10, 11] for an overview on nonholonomic systems and control of wheeled robots.

Prescribed performance (PP) controllers have recently been proposed in order to guarantee the system transient performance. While usually the problems are solved in the sense of asymptotic convergence of the position errors to zero, with the prescribed performance approach the aim is also to achieve system performance in the transient phase. The reader is referred to the recent literature, e.g. [12–14], which however is devoted mainly to robot motion control or holonomic systems. Another way to prescribe the performance of a system is to design controllers that can ensure the exponential convergence of the error to zero and find the relation between the gain values and the system convergence rate. Dealing with a driftless system such as the model considered and just introduced, the usual definition of exponential stability can not be readily applied. This problem has been explored for example in [15], where the control is realized adopting the homogeneous feedback, and also in [16–18]. The problem of exponential stabilization of nonholonomic systems is an additional motivation for introducing prescribed performance concept in the control of these systems.

In this work two prescribed controllers are proposed for the posture regulation of a unicycle nonholonomic system: a) a controller based on polar coordinates that can bind the distance of the unicycle from the desired position, together with the vehicle orientation, and b) a time-varying controller designed in order to guarantee prescribed performance on the orientation. The paper proposes a specific transformation in order to impose prescribed performance bounds on the orientation since theoretical analysis have shown that the more general standard PP transformation leads to unbounded terms in the control inputs and the convergence is no longer guaranteed. Simulations confirm the effectiveness of the proposed solutions as well as their robustness to different types of disturbance. The contributions of this work can be summarized in the following points:

- The proposed control schemes guarantee not only the convergence to the desired posture(thus solving the regulation problem - see e.g. the overview papers [10,11]) but also the fulfilment of prescribed performance constraints. This allows the a priori specification of the rate of convergence without tuning the controller gains.
- The prescribed performance control design (e.g. [14]) is modified in order to deal with a nonholonomic system.
- Given a maximum overshoot and a desired convergence rate, exponential convergence can be achieved but with a simpler and quite intuitive approach as compared to [15].

The rest of the paper is organized as follows: in Section 2 we give a short review of the regulation problem for the unicycle (control with polar coordinates and time-varying laws), and a brief summary of the state of the art for the prescribed performance control. In Section 3 a control law that guarantees prescribed performance on the distance and on the orientation of the unicycle is designed adopting the polar coordinates representation while in Section 4 an extension for the time-varying control law is proposed. The results of the simulations for the new control laws are reported in Section 5 and conclusions follow in Section 6.

2 Preliminaries

2.1 Unicycle models

The reader is referred to e.g. [19–22]. A unicycle is a vehicle with a single orientable wheel. The unicycle is the simplest model of a nonholonomic wheeled mobile robot (WMR) and it corresponds to a single wheel rolling on the plane. The generalized coordinates are $q =$

$(x, y, \theta) \in \mathcal{Q} = \mathbb{R}^2 \times SO^1$: (x, y) are the Cartesian coordinates of the contact point with the ground, measured in the fixed reference frame, and θ is the steering angle. The pure rolling constraint for the unicycle can be expressed in the Pfaffian form as

$$\dot{x}\sin\theta - \dot{y}\cos\theta = [\sin\theta \quad -\cos\theta \quad 0]\dot{q} = 0.$$

The kinematic model of the unicycle can be expressed in the following form:

$$\begin{aligned} \dot{x} &= v\cos\theta \\ \dot{y} &= v\sin\theta \\ \dot{\theta} &= \omega \end{aligned} \tag{1}$$

where the inputs v and ω are, respectively, the *driving velocity* (the linear velocity of the wheel) and the *steering velocity* (the angular velocity of the wheel around the vertical axis).

Different descriptions that yield to different type of control solution have been proposed for posture regulation of the unicycle model. Here we mention the polar coordinates and the time-varying approach, which are also used in our approach:

A convenient way to formulate the regulation problem for a unicycle is to express it in polar coordinates. Consider then the following change of variables:

$$\begin{aligned} r &= \sqrt{x^2 + y^2} \\ \gamma &= \operatorname{atan2}(y, x) - \theta + \pi \\ \delta &= \gamma + \theta. \end{aligned} \tag{2}$$

A graphical representation is illustrated in Fig. 1.

In these coordinates, the kinematic model is expressed as:

$$\begin{aligned} \dot{r} &= -v\cos\gamma \\ \dot{\gamma} &= \frac{\sin\gamma}{r}v - \omega \\ \dot{\delta} &= \frac{\sin\gamma}{r}v, \end{aligned} \tag{3}$$

The reader is referred to [9] for more details. The system (3) can be decoupled in two subsystems, one for the distance (r) and one for the orientation (γ, δ). The linear velocity input can be used directly to regulate the distance to zero; in the literature (e.g. [11]) v is designed as

$$v = r\cos\gamma \tag{4}$$

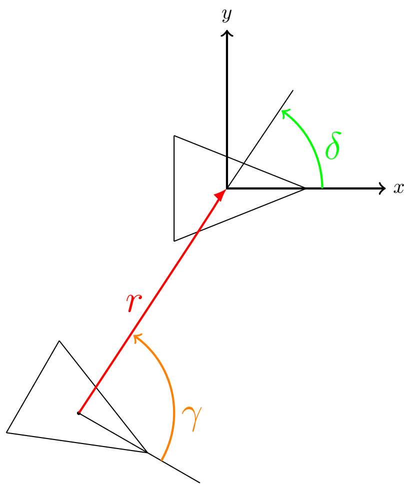

Figure 1: Polar coordinates for the unicycle

so that the subsystem related to the distance $\dot{r} = -v\cos\gamma$ is stabilized. Then, the steering velocity ω is devoted to ensure the stability of the second subsystem describing the orientation following Lyapunov analysis. Therefore, the conventional inputs to control the unicycle described by polar coordinates can be designed as follows:

$$v = k_1 r \cos\theta \tag{5}$$

$$\omega = k_2\gamma + k_1\frac{\sin\gamma\cos\gamma}{\gamma}(\gamma + k_3\delta) \tag{6}$$

where $k_1 > 0$, $k_2 > 0$, $k_3 > 0$ are positive control gains.

When dealing with time-varying control, the following error definition is adopted to design the control inputs:

$$e = \begin{bmatrix} e_1 \\ e_2 \\ e_3 \end{bmatrix} = \begin{bmatrix} \cos\theta & \sin\theta & 0 \\ -\sin\theta & \cos\theta & 0 \\ 0 & 0 & 1 \end{bmatrix} \begin{bmatrix} x_d - x \\ y_d - y \\ \theta_d - \theta \end{bmatrix} \tag{7}$$

and its dynamics can be expressed as

$$\begin{aligned} \dot{e}_1 &= v_d\cos e_3 - v + e_2\omega \\ \dot{e}_2 &= v_d\sin e_3 + e_1\omega \\ \dot{e}_3 &= \omega_d - \omega \end{aligned} \tag{8}$$

Refer to [9] for more details on solution for posture stabilization for nonholonomic WMRs based on time-varying feedback.

2.2 Prescribed performance control

The prescribed performance control technique has been introduced in [23]; see also [13, 14]. The goal of the prescribed performance controller is to guarantee that the error e evolves within certain a priori defined performance bounds described by a decreasing function $\rho(t)$, called *performance function*, and an acceptable overshoot range M.

The performance bounds $\forall t \geq 0$ for each element $e_i,\ i = 1, \ldots, n$ of the error are mathematically defined as:

$$\begin{aligned} -M_i\rho_i(t) < e_i < \rho_i(t), \quad \text{if } e_{i_0} \geq 0, \\ -\rho_i(t) < e_i < M_i\rho_i(t), \quad \text{if } e_{i_0} \leq 0, \end{aligned} \tag{9}$$

where $e_{i_0} = e_i(0),\ i = 1, \ldots, n,\ 0 \leq M_i \leq 1$, and $\rho_i(t)$ is smooth, bounded, strictly positive decreasing function of time and satisfying $\lim_{t\to\infty} \rho_i(t) = \rho_{i\infty} > 0$. The performance function can be defined as:

$$\rho_i(t) = (\rho_{i0} - \rho_{i\infty}) \exp(-L_i t) + \rho_{i\infty}.$$

The parameter $\rho_{i\infty}$ is chosen to be big enough so that it is comparable to the range of measurement noise.

In order to achieve the asymptotic convergence while guaranteeing prescribed performance for nonholonomic systems, an error transformation is used. At first the error is modulated by $\rho_i(t)$, and then a transformation function $T_i(\cdot)$ is applied. The modulated error is defined as follows:

$$\hat{e}_i(t) \triangleq \frac{e_i(t)}{\rho_i(t)}. \tag{10}$$

Then, the transformed error vector $\boldsymbol{\varepsilon}(t) \in \mathbb{R}^n$ is defined through transformation functions $T_i : D_{\hat{e}_i} \to \mathbb{R},\ i = 1, \ldots, n$, so that its components are defined as:

$$\varepsilon_i(t) \triangleq T_i(\hat{e}_i(t)) \tag{11}$$

where the transformations $T_i(\cdot),\ i = 1, \ldots, n$ are smooth, strictly increasing and define increasing bijective mappings of the performance domain:

$$D_{\hat{e}_i} \triangleq \{\hat{e}_i : \hat{e}_i \in (-M_i, 1)\} \quad \text{if } e_{i_0} \geq 0,$$

$$D_{\hat{e}_i} \triangleq \{\hat{e}_i : \hat{e}_i \in (-1, M_i)\} \quad \text{if } e_{i_0} \leq 0.$$

Differentiating (11) with respect to time, the following expression is obtained:

$$\dot{\varepsilon}_i(t) = J_{Ti}(t)[\dot{e}_i + \alpha_i(t)e_i] \tag{12}$$

where $J_{Ti}(t)$ and $\alpha_i(t)$ are respectively

$$J_{Ti}(t) \triangleq \frac{\partial T_i}{\partial \hat{e}_i(t)} \frac{1}{\rho_i(t)} > 0, \quad \alpha_i(t) \triangleq -\frac{\dot{\rho}_i(t)}{\rho_i(t)} > 0.$$

When e_i approaches the prescribed performance bounds, ε_i grows and becomes unbounded. Thus, if from the Lyapunov analysis ε_i is proved bounded ($\varepsilon_i \in \mathcal{L}_\infty$), then the aforementioned transformation is bounded as well and this means that e_i stays within the predefined bounds. To simplify the notation, in what follows ρ_i and α_i will be used, implying the time dependency.

3 Control design for distance and orientation regulation with Prescribed performance guarantees

In this section a control law that guarantees prescribed performance on the distance and on the orientation of the unicycle is designed. Polar coordinates description is considered and bounds are imposed on r and on the angle γ and hence, indirectly, on the orientation of the unicycle ($\theta = \delta - \gamma$). The subscript r will be used for the terms referring to the first polar coordinate transformed by means of *prescribed performance* bounds, and the subscript γ for the terms referring to the homonym angle coordinate. We define

$$\begin{aligned} \rho_r(t) &= (\rho_{r0} - \rho_{r\infty}) \exp(-L_r t) + \rho_{r\infty} \\ \rho_\gamma(t) &= (\rho_{\gamma 0} - \rho_{\gamma\infty}) \exp(-L_\gamma t) + \rho_{\gamma\infty}. \end{aligned} \tag{13}$$

and the quantities $\hat{r} = \dfrac{r}{\rho_r}$, $\hat{\gamma} = \dfrac{\gamma}{\rho_\gamma}$. Consider now the transformations

$$\varepsilon_r = T\left(\hat{r}\right) = \begin{cases} \ln\left(\frac{M_r + \hat{r}}{M_r(1-\hat{r})}\right), & \text{if } r_0 \geq 0 \\ \ln\left(\frac{M_r(1+\hat{r})}{M_r - \hat{r}}\right), & \text{if } r_0 \leq 0, \end{cases} \tag{14}$$

and

$$\varepsilon_\gamma = \operatorname{sign}(\hat{\gamma}) \sqrt{\ln(\cos\hat{\gamma})^{-2}} \tag{15}$$

respectively for r and γ. Define the candidate Lyapunov function as

$$V = \frac{1}{2}\varepsilon_r^2 + \frac{1}{2}\varepsilon_\gamma^2 + \frac{k_3}{2}\delta^2 \tag{16}$$

in order to design the following control law:

$$v = k_1 J_r \varepsilon_r \cos\gamma + k_3 \alpha_r r \cos\gamma \tag{17}$$

$$\omega = k_2 \tan\hat{\gamma} + \alpha_\gamma \gamma + \rho_\gamma \Big(k_3 \delta + \frac{\tan\hat{\gamma}}{\rho_\gamma}\Big)\Big(k_1 J_r \frac{\varepsilon_r}{r} + \alpha_r\Big) \cos\hat{\gamma} \cos\gamma \frac{\sin\gamma}{\sin\hat{\gamma}} \tag{18}$$

where k_1, k_2, k_3 are positive control gains and $\alpha_r, \alpha_\gamma, \rho_r, \rho_\gamma, J_r$ are defined as in section 2.2.

Note that $\frac{1}{2}\varepsilon_\gamma^2$ equals $-\ln\cos\hat{\gamma}$, and this expression leads to formulate a control law depending not directly on ε_γ but on $\tan\hat{\gamma}$. The range of values where ε_γ is well defined is $\hat{\gamma} \in (-\frac{\pi}{2}, \frac{\pi}{2})$, that is $\gamma \in (-\frac{\pi}{2}\rho_\gamma, \frac{\pi}{2}\rho_\gamma)$. This range is time-varying following the rate of convergence of ρ_γ. Also, if $\gamma_0 \in (-\frac{\pi}{2}\rho_{\gamma 0}, \frac{\pi}{2}\rho_{\gamma 0})$, then this angle coordinate will evolve within the predefined set of value, without ever leaving it.

Remark To impose bounds on r, the approach proposed in [12], can be directly applied adopting a transformation defined e.g. as (14). A possible feasible transformation on γ that allows to impose prescribed bounds on the vehicle orientation is the one in (15), while the typical transformation of the form (14) can not be applied to achieve the two control objectives. The transformation must be chosen in order to guarantee that the new control inputs satisfy the following properties:

(P1) each input must be bounded;

(P2) the first derivative with respect to time of each input must be bounded.

The second condition is needed since the convergence proof exploits Barbalat's lemma. Therefore, it is remarkable that exploiting a transformation of the type (14) the property (P1) is satisfied, but (P2) is not. On the other hand, adopting the transformation (15), both (P1) and (P2) are satisfied. Thus, the control velocities (17-18) are well defined and satisfy (P1) and (P2). ■.

The designed control law guarantees the convergence to the desired position and orientation while satisfying the predefined bounds as it is proved in the following theorem:

Theorem 1. *Consider the polar coordinate description (3) of the unicycle and the feedback control (17-18) with k_1, k_2, k_3 positive constants. The closed-loop system (3)-(17-18) is then globally asymptotically stabilized to the posture $(r, \gamma, \delta) = (0, 0, 0)$. Also, the polar coordinates r and γ respect the prescribed limits.*

Proof: The control inputs (17-18) are well defined and bounded. More specifically, $\frac{\varepsilon_r}{r}$ is bounded as long as r stays away from zero and converges to the finite value $E_r = \dfrac{1+M}{\rho_r M}$ as $r \to 0$; $\dfrac{\sin\gamma}{\sin\hat{\gamma}}$ is bounded as long as $\hat{\gamma}$ stays away from zero and converges to the finite value $\rho_\gamma(t)$ as γ (or in the same way $\hat{\gamma}$) tends to zero. Substituting the designed controller in $\dot{V}$ we have

$$\dot{V} = -k_1\varepsilon_r^2 J_r^2 \cos^2\gamma - \frac{k_2}{\rho_\gamma}\tan^2\hat{\gamma} \le 0. \tag{19}$$

The proof for the convergence of the coordinates can be carried on by exploiting Barbalat's Lemma.

Specifically, equation (19) implies that the state is bounded, $\dot{V}(t)$ is uniformly continuous since $\ddot{V}(t)$ is bounded, and $V(t)$ tends to a limit value. By Barbalat's lemma, $\dot{V}(t)$ tends to zero and thus also ε_r and $\hat{\gamma}$ do (and hence r and γ also). Analyzing the closed-loop system, note that $\dot{r}$ and $\dot{\delta}$ converge to zero and δ converges to a finite limit; $\dot{\gamma}$ tends to a finite limit also and it is uniformly continuous since $\ddot{\gamma}$ is bounded. To prove that $\ddot{\gamma}$ is bounded notice that all its terms are bounded. In particular, for the term $\dot{\omega}$ we have that

$$\frac{d}{dt}\frac{\sin\gamma}{\sin\hat{\gamma}} = \left[\frac{\cos\gamma}{\sin\hat{\gamma}} - \frac{1}{\rho_\gamma}\frac{\sin\gamma}{\sin\hat{\gamma}}\frac{\cos\hat{\gamma}}{\sin\hat{\gamma}}\right]\dot{\gamma} + \alpha\frac{\hat{\gamma}}{\sin\hat{\gamma}}\frac{\sin\gamma}{\sin\hat{\gamma}}\cos\hat{\gamma} \tag{20}$$

The second term is well defined and bounded, while the term in the squared brackets

$$\frac{\cos\gamma}{\sin\hat{\gamma}} - \frac{1}{\rho_\gamma}\frac{\sin\gamma}{\sin\hat{\gamma}}\frac{\cos\hat{\gamma}}{\sin\hat{\gamma}}$$

is bounded as $\hat{\gamma} \neq 0$, and it tends to zero as $\hat{\gamma} \to 0$. Eventually, $\ddot{\gamma}$ is bounded, $\dot{\gamma}$ is uniformly continuous and tends to zero. Hence we can conclude that all the coordinates converge to zero. From the previous analysis, ε_r and ε_γ are proved bounded. Thus, r and γ are guaranteed to respect the predefined bounds. □

4 Extension for Time-varying control

Consider the error dynamics defined in (8) and the feedback control law

$$\begin{aligned} v &= v_d \cos e_3 - u_1 \\ \omega &= \omega_d - u_2, \end{aligned} \tag{21}$$

with u_1, u_2 the inputs to be designed. The conventional time-varying control law is designed as follows:

$$u_1 = -k_1(v_d(t), \omega_d(t))e_1 \tag{22}$$

$$u_2 = -\bar{k}_2 v_d(t)\frac{\sin e_3}{e_3}e_2 - k_3(v_d(t), \omega_d(t))e_3 \tag{23}$$

where $k_1, \bar{k}_2, k_3$ are positive control gains.

In order to achieve fast convergence and set narrow bounds on the orientation, introduce a time varying transformation through the modulating function $\rho(t)$, such that

$$e_3 \quad \mapsto \quad \hat{e}_3 = \frac{e_3}{\rho}$$

Define the Lyapunov function as

$$V = \frac{k_2}{2}\left(e_1^2 + e_2^2\right) + \frac{k_3}{2}\varepsilon_3^2 \tag{24}$$

where $\varepsilon_3 \triangleq \mathrm{sign}(\hat{e}_3)\sqrt{\ln(\cos\hat{e}_3)^{-2}}$. Note that the range of values where ε_3 is well defined is $\hat{e}_3 \in (-\frac{\pi}{2}, \frac{\pi}{2})$, that is $e_3 \in (-\frac{\pi}{2}\rho, \frac{\pi}{2}\rho)$. This range is time-varying following the rate of convergence of ρ. Also, if $e_{30} \in (-\frac{\pi}{2}\rho_0, \frac{\pi}{2}\rho_0)$, then this angle coordinate will evolve within the predefined set of values, without ever leaving it.

Define the input controllers

$$u_1 = -k_1 e_1 \tag{25}$$

$$u_2 = -e_3\alpha(t) - \frac{k_2\rho}{k_3} v_d e_2 \frac{\cos\hat{e}_3}{\sin\hat{e}_3}\sin e_3 - \tan\hat{e}_3. \tag{26}$$

where k_1, k_2, k_3 are positive control gains and α and ρ are defined as in section 2.2. Differentiating V with respect to time, substituting the designed controllers in (25)-(26) and canceling out some terms yields:

$$\dot{V} = -k_1 k_2 e_1^2 - \frac{k_3}{\rho}\tan^2\hat{e}_3 \leq 0. \tag{27}$$

Hence we can use V in order to prove the following theorem:

Theorem 2. *Consider the unicycle (1), the error dynamics (8) and the feedback control (21) with control inputs defined as (25)-(26) and k_1, k_2, k_3 positive constants. The closed-loop system (1)-(21) is then globally asymptotically stabilized to the posture $(x, y, \theta) = (0, 0, 0)$. Also, the error component e_3 respects the prescribed limits.*

Proof: The first derivative of the Lyapunov function (24) is given by

$$\dot{V} = k_2 e_1 u_1 + k_2 e_2 \sin e_3 v_d + k_3 \frac{\sin\hat{e}_3}{\cos\hat{e}_3}\frac{u_2 + e_3\alpha(t)}{\rho}. \tag{28}$$

Substituting the designed controllers (25)-(26) in (27) and canceling out some terms we obtain (27). The proof for the convergence of the error components and for the Cartesian coordinates can be carried on exploiting Barbalat's Lemma. In order to exploit Barbalat's Lemma, let us check the second derivative of e_3:

$$\ddot{e}_3 = \dot{u}_2 = -e_3\dot{\alpha}(t) - \frac{k_2\rho}{k_3}\Big[\dot{v}_d e_2 \frac{s_{e_3}}{t_{\hat{e}_3}} + v_d \dot{e}_2 \frac{s_{e_3}}{t_{\hat{e}_3}} + \underline{v_d e_2 \frac{d}{dt}\Big(\frac{s_{e_3}}{t_{\hat{e}_3}}\Big)}\Big] - \big(1 + t_{\hat{e}_3}^2\big)\dot{\hat{e}}_3 +$$
$$-\frac{k_2\dot{\rho}(t)}{k_3} v_d e_2 \frac{\cos\hat{e}_3}{\sin\hat{e}_3}\sin e_3 - \big(1 + \tan^2\hat{e}_3\big)\dot{\hat{e}}_3.$$

where $s_{e_3}, c_{e_3}, t_{e_3}$ indicate respectively $\sin e_3, \cos e_3, \tan e_3$. The derivative of $\hat{e}_3$ is

$$\dot{\hat{e}}_3 = \frac{1}{\rho}u_2 + \alpha(t)\hat{e}_3$$

and the underlined term, in this case, can be written as

$$\frac{d}{dt}\Big(\frac{\sin e_3}{\sin\hat{e}_3}\cos\hat{e}_3\Big)$$

while

$$\frac{d}{dt}\frac{\sin e_3}{\sin\hat{e}_3} = \Big[\frac{\cos e_3}{\sin\hat{e}_3} - \frac{1}{\rho}\frac{\sin e_3}{\sin\hat{e}_3}\frac{\cos\hat{e}_3}{\sin\hat{e}_3}\Big]u_2 + \alpha\hat{e}_3\frac{\sin e_3}{\sin\hat{e}_3}\frac{\cos\hat{e}_3}{\sin\hat{e}_3}. \tag{29}$$

The term in the square brackets in (29) is bounded as $\hat{e}_3 \neq 0$, and it tends to zero as $\hat{e}_3 \to 0$. Also, $\dot{e}_3 = u_2$ is bounded, as previously discussed. Also the term

$$\hat{e}_3\frac{\sin e_3}{\sin\hat{e}_3}\frac{\cos\hat{e}_3}{\sin\hat{e}_3} = \frac{\hat{e}_3}{\sin\hat{e}_3}\frac{\sin e_3}{\sin\hat{e}_3}\cos\hat{e}_3$$

is well defined and bounded. Thus, equation (27) implies that the state is bounded, $\dot{V}$ is uniformly continuous and V tends to a limit value. By Barbalat's Lemma, $\dot{V}$ tends to zero and also e_1 and $\hat{e}_3$ do. From the analysis of the closed-loop system and the boundedness of $\ddot{e}_3$, and by Barbalat's Lemma, it is possible to conclude that all the error components converge to zero. Also, from the previous analysis, ε_3 is proved bounded. Thus, e_3 is guaranteed to respect the predefined bounds. □

5 Simulations

Matlab simulations for the control of the unicycle designed with polar coordinates are reported in Figures 2-4. Figure 2 shows the bounded coordinate behavior together with the bounds defined by the modulating functions ρ_γ and ρ_r, pointing out that these bounds are fully satisfied. The vehicle motion is depicted in Figure 2.c. In Figure 3, the coordinates convergence is shown. Note that the convergence achieved with the control law (17-18) is much faster than the convergence obtained applying the conventional control law (5)-(6). In Figure 4 it is possible to compare the inputs needed to drive the vehicle to the desired posture, on equal convergence rate. Note that the initial velocities are greater in the case that the conventional controller is used. Also, applying the control law designed in order to guarantee prescribed performance on both position and orientation, the obtained inputs and coordinates evolutions are smoother and better distributed over the time. All the control gains are reported in figure captions.

The proposed control law (17-18) is also robust to disturbances. Figure 7 depicts the unicycle behaviour in presence of an additive disturbance of the steering velocity, that is $\omega = \omega_{des} + \delta$, where ω_{des} represents the designed law and δ is the additive constant disturbance, taken equal to 1. The same type of disturbance is used in other studies, e.g. in [24]. The advantage of the proposed controller as compared to the conventional is inferred by comparing the results in Figure 7. Figure 9 depicts the unicycle behaviour in presence of frequency shifts in both the velocity inputs. In simulation, the driving and steering velocity are multiplied by a filter to obtain frequency shifted signals, so that the input velocities are $e^{-at}v(t)$ and $e^{-bt}\omega(t)$ ($a = 0.5, b = 0.8$ in the simulation depicted in Figure 9). The convergence of the coordinates and the fulfilment of the prescribed bounds are guaranteed.

Matlab simulation for the control of the unicycle with time-varying law is reported in Figure 5-6. The oscillating behavior is an intrinsic characteristic of driving the unicycle with time-varying laws. Prescribed performance control does not require demanding tuning procedures, since it is defined setting just the desired rate of convergence and maximum overshoot. Tuning processes are adopted in order to compare different behaviors and bounds. All the control gains are reported in figure captions.

The control law (21) with the proposed control inputs defined as (25)-(26) is also robust to disturbances. Small random additive perturbations in both the velocity inputs have been added in the simulation scenario. The perturbations are of 10^{-2} order of size. A steady state error remains for coordinate convergence due to the additive disturbance. However, the effect on the coordinate convergence is less relevant when the proposed controller is applied, while e_3 still fulfils the PP bounds. Figure 10 depicts the unicycle behaviour in presence of disturbances. The fulfilment of the prescribed bounds are guaranteed while the error on the coordinates remain bounded. The advantage of the proposed controller as compared to the conventional is inferred by comparing the results in Figure 10 (referring to the proposed control law) and in Figure 11 (referring to the conventional controller).

6 Conclusion

This paper addresses the regulation problem for mobile robots of the type of the unicycle by designing control schemes that guarantee prescribed performance guaranties. Two main approaches to solve the regulation problem for the unicycle are employed (control with polar coordinates and time-varying control) and have been combined with the prescribed performance control concept. The main results and proofs of convergence have been obtained with Lyapunov analysis. The study also illustrates a specific transformation, needed given the nonholonomic structure of the system. In fact, specific properties have to be satisfied in order to choose a feasible transformation on the orientation angle coordinates that can bind the unicycle orientation. Simulation results demonstrate the theoretical findings and show the advantage of proposed controllers in terms of performance and control input profiles over the classical design approaches.

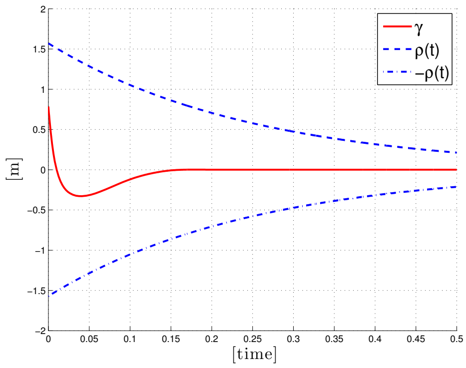

(a) γ stays in the bounds designed by the modulating function $\rho_\gamma(t)$

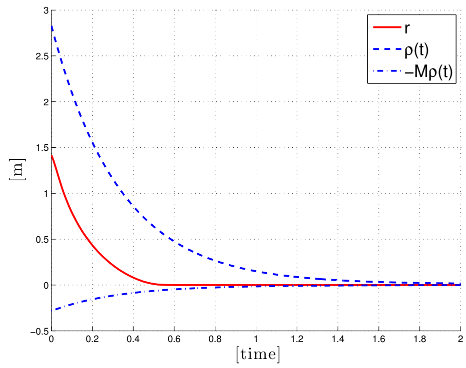

(b) r stays in the bounds designed by the modulating function $\rho_r(t)$

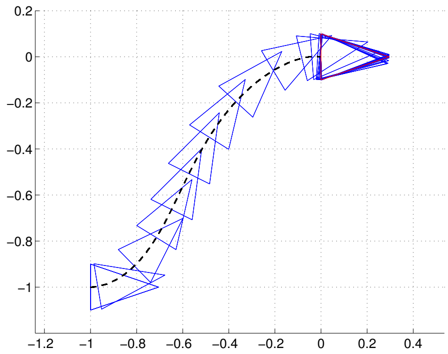

(c) Unicycle behavior

Figure 2: Unicycle behavior. Settings: $(x_0, y_0, \theta_0) = (-1, -1, 0)$ (m,m,rad). $(k_1, k_2, k_3) = (0.1, 3, 2)$, $\rho_{0_\gamma} = \pi/2$, $\rho_{\infty_\gamma} = 0.0001$, $L_\gamma = 4$; $\rho_{0_r} = 2|r_0|$, $\rho_{\infty_r} = 0.01$, $L_r = 3$, $M_r = 0.1$;

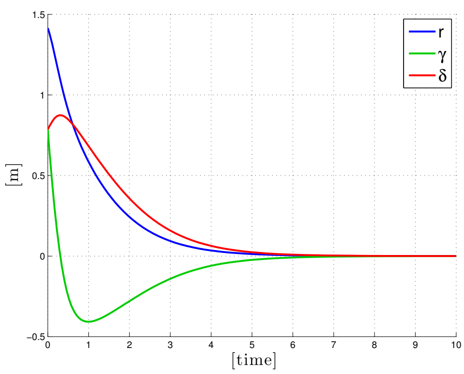

(a) Conventional controller

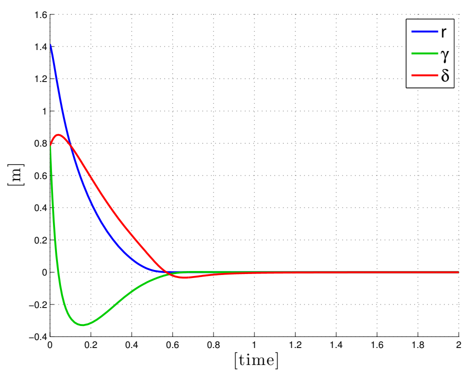

(b) Controller with PP

Figure 3: Coordinate convergence. Figure (a) refers to the control law in eq. (5)-(6) with $(k_1, k_2, k_3) = (1, 3, 2)$; Figure (b) refers to the experiment in Figure 2 corresponding to the modified controller in eq. (17)-(18).

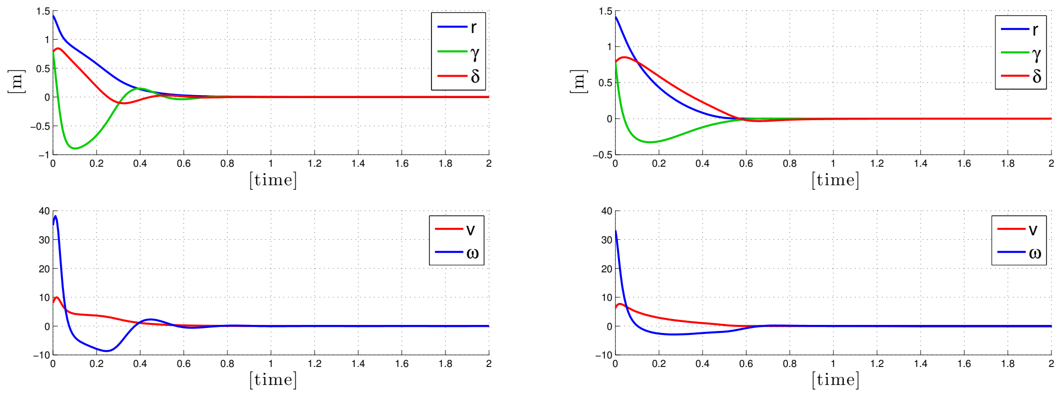

(a) conventional control law

(b) Control law guaranteeing PP bounds on r and γ

Figure 4: Inputs comparison, on equal convergence rate. Figure (a) refers to the control law in eq. (5)-(6), now with $(k_1, k_2, k_3) = (8, 14, 5)$ to satisfy the constraint of the convergence rate; Figure (b) refers to the experiment in Figure 2 corresponding to the modified controller in eq. (17)-(18).

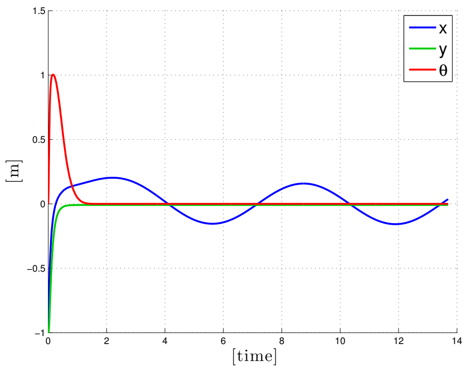

(a) Coordinates x, y, θ

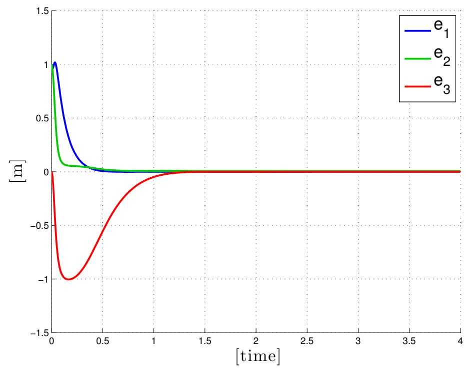

(b) Errors e_1, e_2, e_3

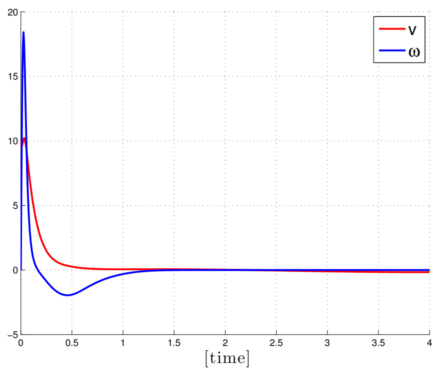

(c) Input velocities v, ω

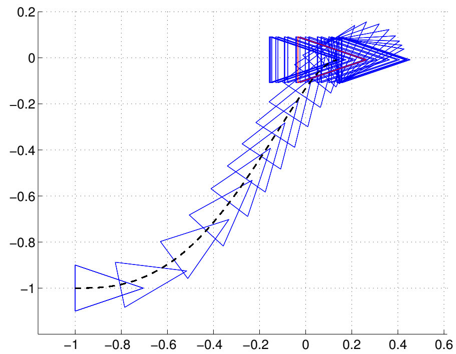

(d) Unicycle behavior

Figure 5: Unicycle behavior with the proposed time-varying control law. Desired linear velocity designed with heating function. Settings: $(x_0, y_0, \theta_0) = (-1, -1, 0)$ (m,m,rad). $(k_1, k_2, k_3, k_4, k_5) = (10, 50, 0.1, 0.8, 70)$. $\rho_0 = \pi/2, \rho_\infty = 0.01,\ L = 2$.

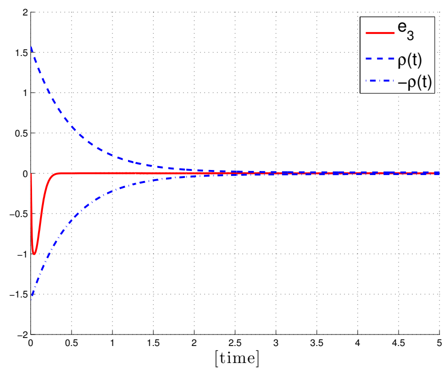

Figure 6: Bounds on e_3. Unicycle behavior with time-varying control law. Desired linear velocity designed with heating function. Settings: $(x_0, y_0, \theta_0) = (-1, -1, 0)$ (m,m,rad). $(k_1, k_2, k_3, k_4, k_5) = (10, 50, 0.1, 0.8, 70)$.

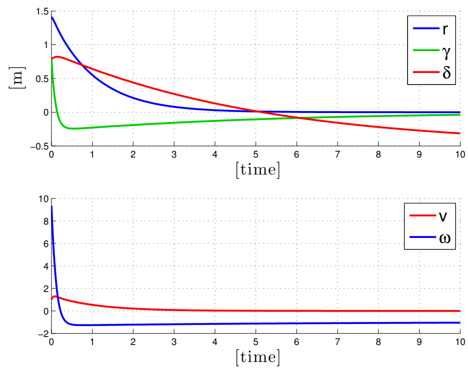

(a) Coordinates and Velocities - conventional controller

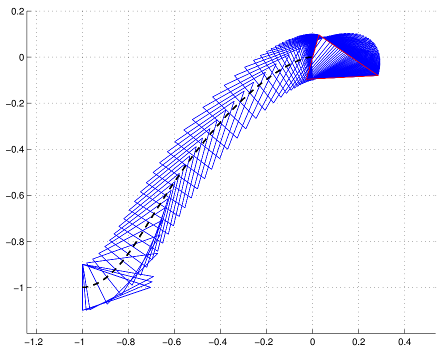

(b) Unicycle behavior - conventional controller

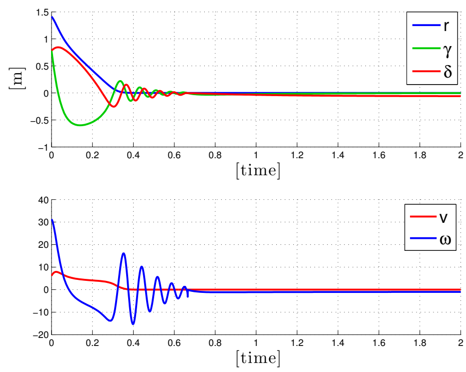

(c) Coordinates and Velocities - proposed controller

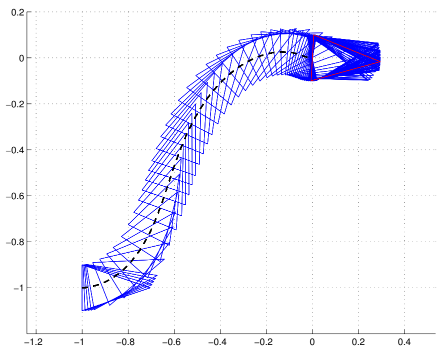

(d) Unicycle behavior - proposed controller

Figure 7: Robustness evaluation: comparison between the behavior of the unicycle driven by the conventional control law in eq. (5)-(6) - Figures (a) and (b) - and the behavior of the unicycle driven by the proposed control law in eq. (17)-(18) - Figures (c) and (d). An additive disturbance $\delta = 1$ is applied to the steering velocity. Control gains have been chosen equals for the two controllers: $(k_1, k_2, k_3) = (1, 10, 2)$. It is possible to note that the results are affected by a steady state error. However, the system controlled by the proposed law is less affected compared to the system controlled by the conventional controller; the error on coordinate convergence in the case of the PP controller is much smaller.

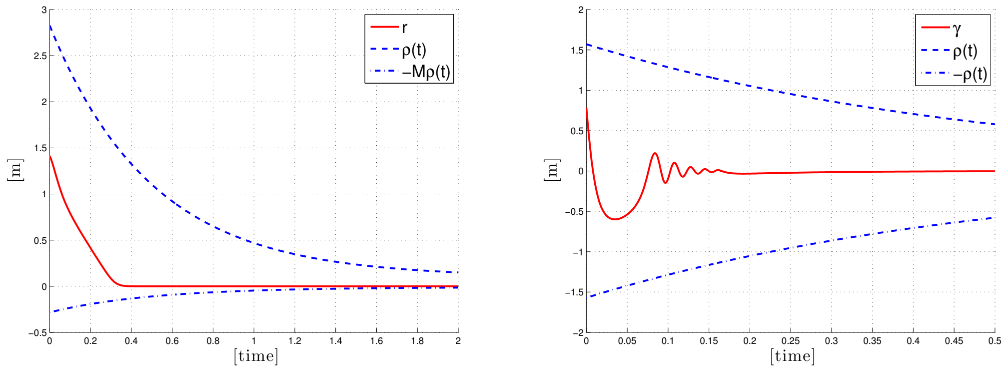

(a) Fulfilment of PP bounds on r

(b) Fulfilment of PP bounds on γ

Figure 8: Robustness evaluation: the fulfilment of PP bounds is guaranteed in the scenario presented in Fig. 7.

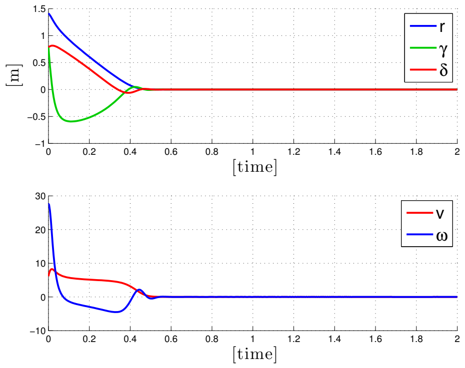

(a) Coordinates and Velocities

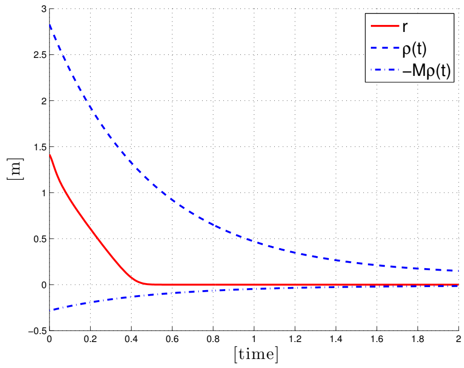

(b) Fulfilment of PP bounds on r

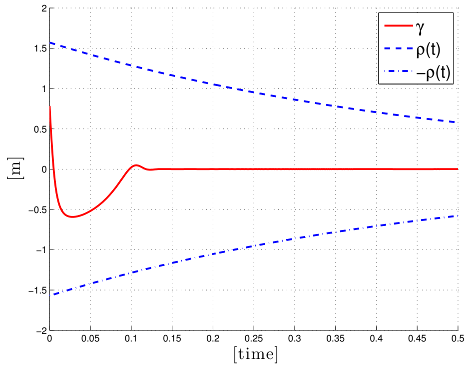

(c) Fulfilment of PP bounds on γ

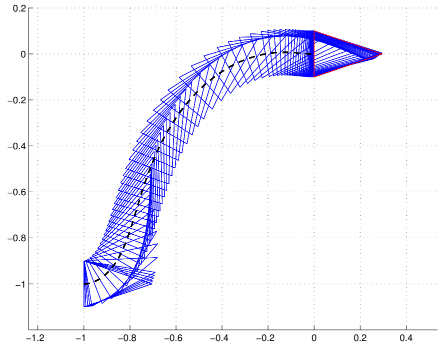

(d) Unicycle behavior

Figure 9: Robustness evaluation: behavior of the unicycle driven by the proposed control law in eq. (17)-(18), with frequency shifts on both the driving and steering velocity. Control gains have been kept as in the previous simulations. Some of the PP parameters have been slightly relaxed: $\rho_{\infty_\gamma} = 0.01$, $L_\gamma = 2$; $\rho_{\infty_r} = 0.1$, $L_r = 2$ while the same values have been taken for the remaining parameters.

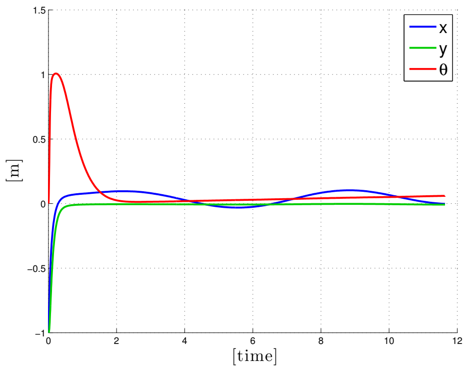

(a) Coordinates

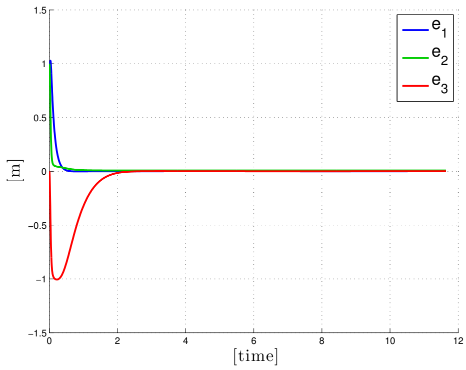

(b) Errors

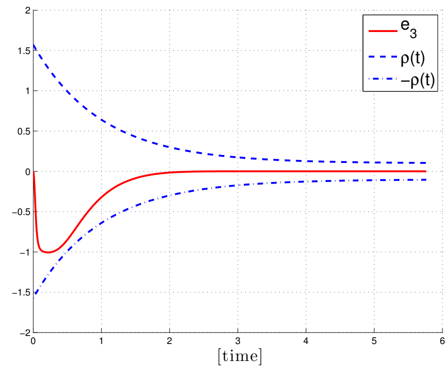

(c) Fulfilment of PP bounds on e_3

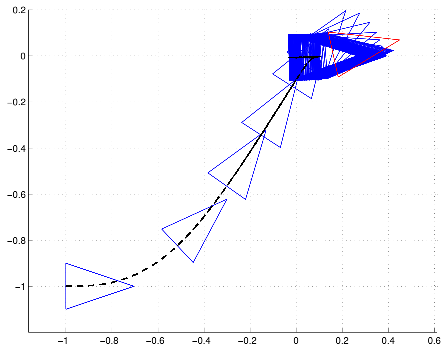

(d) Unicycle behavior

Figure 10: Robustness evaluation: behavior of the unicycle driven by the proposed time-varying control law in eq. (21) with control inputs defined as (25)-(26). Additive random disturbances are applied to both the steering and driving velocity. Control gains have been kept as in the previous simulations while PP parameters have been slightly relaxed: $\rho_0 = \pi/2, \rho_\infty = 0.1, \; L = 1$.

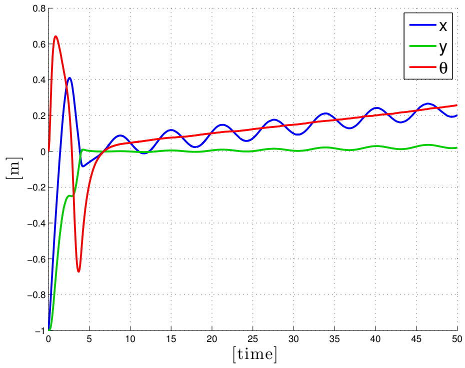

(a) Coordinates

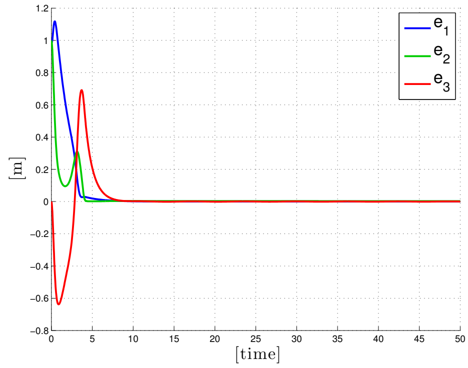

(b) Errors

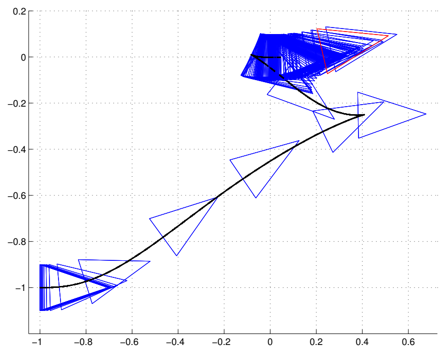

(c) Unicycle behavior

Figure 11: Robustness evaluation: behavior of the unicycle driven by the conventional time-varying control law in eq. (21) with control inputs defined as (22)-(23). The scenario is the same as described in Figure 10, with random additive disturbances on the velocity inputs. Control gains have been kept as in the previous simulations.

References

[1] R. W. Brockett *et al.*, *Asymptotic stability and feedback stabilization.* Defense Technical Information Center, 1983.

[2] A. Astolfi, "Discontinuous control of nonholonomic systems," *Systems & Control Letters*, vol. 27, no. 1, pp. 37–45, 1996.

[3] G. Oriolo, A. De Luca, and M. Vendittelli, "WMR control via dynamic feedback linearization: design, implementation, and experimental validation," *IEEE Transactions on Control Systems Technology,*, vol. 10, no. 6, pp. 835–852, 2002.

[4] H. G. Tanner and K. J. Kyriakopoulos, "Discontinuous backstepping for stabilization of nonholonomic mobile robots," *IEEE International Conference on Robotics and Automation. ICRA'02.*, vol. 4, pp. 3948–3953, 2002.

[5] H. G. Tanner, S. Loizou, and K. J. Kyriakopoulos, "Nonholonomic stabilization with collision avoidance for mobile robots," *IEEE/RSJ International Conference on Intelligent Robots and Systems.*, vol. 3, pp. 1220–1225, 2001.

[6] S. Blažič, "A novel trajectory-tracking control law for wheeled mobile robots," *Robotics and Autonomous Systems*, vol. 59, no. 11, pp. 1001–1007, 2011.

[7] S. Blažic, "On periodic control laws for mobile robots," *IEEE transactions on industrial electronics*, vol. 61, no. 7, 2014.

[8] C. Samson, "Control of chained systems application to path following and time-varying point-stabilization of mobile robots," *IEEE Transactions on Automatic Control,*, vol. 40, no. 1, pp. 64–77, 1995.

[9] L. Sciavicco and B. Siciliano, "Modelling and control of robot manipulators." (Springer Verlag, 2000).

[10] I. Kolmanovsky and N. H. McClamroch, "Developments in nonholonomic control problems," *Control Systems, IEEE*, vol. 15, no. 6, pp. 20–36, 1995.

[11] A. De Luca, G. Oriolo, and M. Vendittelli, "Control of wheeled mobile robots: An experimental overview." (Springer, 2001), pp. 181–226.

[12] Y. Karayiannidis and Z. Doulgeri, "Model-free robot joint position regulation and tracking with prescribed performance guarantees," *Robotics and Autonomous Systems*, vol. 60, no. 2, pp. 214–226, 2012.

[13] Z. Doulgeri and Y. Karayiannidis, "PID type robot joint position regulation with prescribed performance guaranties," *IEEE International Conference on Robotics and Automation (ICRA)*, pp. 4137–4142, 2010.

[14] C. Bechlioulis, Z. Doulgeri, and G. Rovithakis, "Prescribed performance adaptive control for robot force/position tracking," *Control Applications,(CCA) & Intelligent Control,(ISIC)*, pp. 920–925, 2009.

[15] R. T. M'closkey and R. M. Murray, "Exponential stabilization of driftless nonlinear control systems using homogeneous feedback," *IEEE Transactions on Automatic Control,*, vol. 42, no. 5, pp. 614–628, 1997.

[16] C. C. De Wit and O. Sordalen, "Exponential stabilization of mobile robots with nonholonomic constraints," *IEEE Transactions on Automatic Control,*, vol. 37, no. 11, pp. 1791–1797, 1992.

[17] C. C. De Wit, H. Khennouf, C. Samson, and O. Sordalen, "Nonlinear control design for mobile robots," *Recent trends in mobile robots*, vol. 11, pp. 121–156, 1993.

[18] J.-M. Coron, "Global asymptotic stabilization for controllable systems without drift," *Mathematics of Control, Signals and Systems*, vol. 5, no. 3, pp. 295–312, 1992.

[19] H. G. Tanner and K. J. Kyriakopoulos, "Nonholonomic motion planning for mobile manipulators," *IEEE International Conference on Robotics and Automation. ICRA'00.*, vol. 2, pp. 1233–1238, 2000.

[20] A. M. Bloch, M. Reyhanoglu, and N. H. McClamroch, "Control and stabilization of nonholonomic dynamic systems," *IEEE Transactions on Automatic Control,*, vol. 37, no. 11, pp. 1746–1757, 1992.

[21] A. De Luca and G. Oriolo, "Modeling and control of nonholonomic mechanical systems," *Kinematics and Dynamics of Multi-Body Systems, CISM Courses and Lectures*, vol. 360, pp. 277–342, 1995.

[22] B. Siciliano, L. Sciavicco, L. Villani, and G. Oriolo, *Robotics: Modelling, Planning and Control*, (1st ed. Springer Publishing Company, Incorporated, 2008).

[23] C. P. Bechlioulis and G. A. Rovithakis, "Robust adaptive control of feedback linearizable mimo nonlinear systems with prescribed performance," *IEEE Transactions on Automatic Control,*, vol. 53, no. 9, pp. 2090–2099, 2008.

[24] D. Buccieri, D. Perritaz, P. Mullhaupt, Z.-P. Jiang, and D. Bonvin, "Velocity-scheduling control for a unicycle mobile robot: theory and experiments," *Robotics, IEEE Transactions on*, vol. 25, no. 2, pp. 451–458, 2009.